A Novel Frequency-Hopping Spread-Spectrum Multiple-Access Network Using M-ary Orthogonal Walsh Sequence Keying

Joonyoung Cho, Youhan Kim, *Student Member, IEEE*, and Kyungwhoon Cheun, *Member, IEEE*

***Abstract*—A novel frequency-hop spread-spectrum multiple-access network employing M-ary orthogonal Walsh sequence keying with noncoherent demodulation is proposed. The transmitted Walsh sequence is overlaid by a user-specific pseudonoise sequence to reduce the effect of multiple-access hits. Two Gaussian approximations for the multiple-access interference from both the dehopped slot and its neighboring slots are developed and are used to analyze the performance of the proposed network for synchronous and asynchronous hopping under nonfading and Rayleigh fading channels. The effect of imperfect hop timing synchronization at the receiver is also analyzed. It is shown that the proposed network offers significantly improved network throughput compared to networks based on traditional M-ary frequency-shift keying modulation.**

***Index Terms*—Error analysis, frequency-hop communication, multiaccess communication, pseudonoise coded communication, spread-spectrum communication.**

I. Introduction

In FREQUENCY-HOP spread-spectrum multiple-access (FHSS-MA) networks, reducing the probability of hits caused by multiple-access interference (MAI) and reducing the error probability given a hit are of utmost importance. These two probabilities are closely related to the modulation scheme employed for each hop. In this paper, we focus on FHSS-MA networks employing M-ary orthogonal modulation with *noncoherent* demodulation and propose an efficient modulation scheme based on Walsh sequences. The proposed modulation scheme, while requiring bandwidth approximately identical to that of traditional M-ary frequency-shift keying (MFSK), significantly improves network performance.

Many of the previous works on FHSS-MA networks employing noncoherent M-ary orthogonal modulation have concentrated on traditional MFSK [1]–[4] or hybrid direct-sequence (DS)-MFSK [5], [6]. Since traditional MFSK by itself does not possess any multiple-access capability, the error probability given a hop is hit is very high. The performance of FHSS-MA networks employing MFSK has been extensively investigated in [1]–[4]. In order to reduce the performance degradation due to multiple-access hits, hybrid DS-MFSK has been considered where further DS spreading is performed on the MFSK modulated signals [5], [6]. However, the additional bandwidth expansion due to DS spreading drastically reduces the number of available frequency-hop slots for a given radio frequency (RF) bandwidth. Hence, such a system may only be applicable to networks with sufficiently large RF bandwidths. Performance of networks employing hybrid DS-MFSK without spectral overlap between the DS-spread MFSK tones within a frequency-hop slot was investigated in [5]. In [6], the issue of optimal separation between the DS-spread MFSK tone frequencies was investigated. Even with optimal tone separation and spectral overlap, the resulting bandwidth of each of the frequency-hop slots is still significantly larger than that of traditional MFSK.

On a different note, FHSS-MA networks based on bandwidth-efficient modulation schemes were proposed in [8]–[10]. These schemes attempt to increase the network performance by increasing the number of frequency-hop slots for a given RF bandwidth, thus decreasing the hit probability. For example, with multiple-carrier on–off keying (MC-OOK) proposed in [8], $\log_2 M$ binary information bits are OOK modulated onto $\log_2 M$ orthogonal carriers. For a given bit rate and modulation order M, MC-OOK reduces the required bandwidth per frequency-hop slot by a factor of $(\log_2 M)/M$ compared with traditional MFSK. At the receiver, a decision is made by comparing the $\log_2 M$ energy detector outputs to a threshold. Unfortunately, the optimum value of the threshold is not only a function of the signal and the noise powers, but also the number of users in the network. Hence, the receiver must adapt its decision threshold, especially for asynchronous hopping, to track the signal-to-noise ratio (SNR) and the number of users.

In this paper, we propose an FHSS-MA network employing a pseudonoise (PN) sequence-overlaid M-ary orthogonal Walsh sequence keying (PN-MWSK) with noncoherent demodulation. In PN-MWSK, a modulation symbol is composed of one of M-ary Walsh sequences overlaid by a user-specific PN sequence with chip rate identical to that of the Walsh sequence. With use of a square-root raised cosine chip pulse shape, the 3-dB bandwidth of PN-MWSK is M/T_s, where T_s is the

Paper approved by J. Wang, the Editor for Wireless Spread Spectrum of the IEEE Communications Society. Manuscript received March 20, 2002; revised October 15, 2002; February 27, 2003; and May 18, 2003. This work was supported in part by HY-SDR Research Center at Hanyang University, Seoul, Korea, under the ITRC Program of MIC, Korea, and in part by the Ministry of Education of Korea through its BK21 Program. This paper was presented in part at the IEEE 52nd Vehicular Technology Conference, Boston, MA, Oct. 2000.

J. Cho was with the Division of Electrical and Computer Engineering, Pohang University of Science and Technology (POSTECH), Pohang, Kyungbuk 790-784, Republic of Korea. He is now with Samsung Electronics Co., Ltd., Republic of Korea.

Y. Kim and K. Cheun are with the Division of Electrical and Computer Engineering, Pohang University of Science and Technology (POSTECH), Pohang, Kyungbuk 790-784, Republic of Korea (e-mail: cheun@postech.ac.kr).

Digital Object Identifier 10.1109/TCOMM.2003.818090

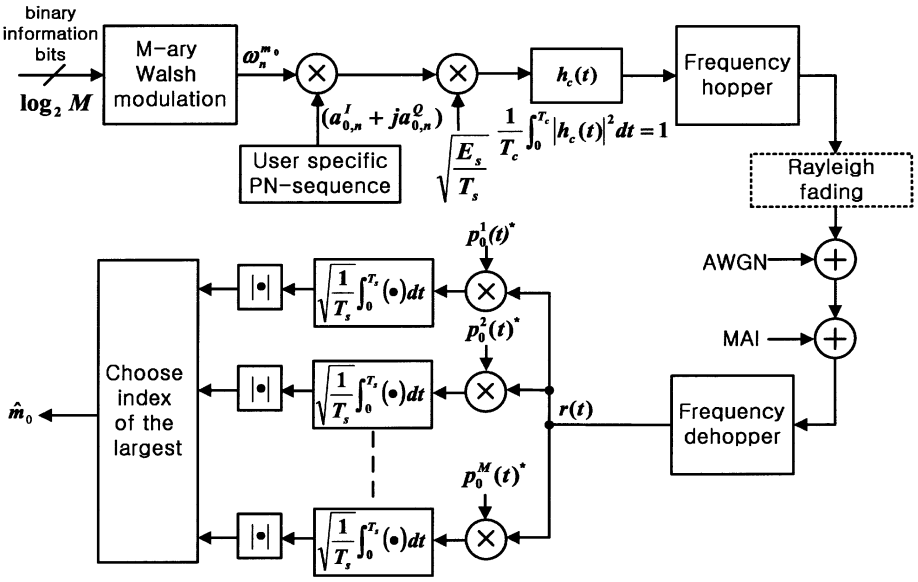

Fig. 1. Proposed system model.

symbol duration. As for traditional MFSK with the frequency separation between contiguous MFSK tones of $1/T_s$, the 3-dB bandwidth for $M = 2$ is approximately $(0.97M)/T_s$, and converges to M/T_s with increasing M. Therefore, both PN-MWSK and traditional MFSK require approximately same bandwidth per frequency-hop slot. Thus, the use of PN-MWSK instead of traditional MFSK does not reduce the number of available frequency-hop slots for a given RF bandwidth. The receiver makes a decision on the transmitted symbol by selecting the index of the largest among the M energy detector outputs. Thus, unlike MC-OOK, there is no need for demodulator parameter optimization as a function of SNR or network load.

In analyzing the performance of the proposed scheme, we accurately take into account the effect of hits to neighboring frequency-hop slots. This spillover effect of interference caused by interfering users hopping to neighboring frequency-hop slots was usually neglected in previous analyses [1]–[7]. Two Gaussian approximations (GAs) are derived for the MAI contributions to the decision variables. The first approximation is given by a simple closed-form expression, but lacks accuracy in nonfading channels for small error probabilities. The second approximation is accurate for all cases considered, but requires numerical averaging.

Performance of the proposed network employing PN-MWSK is analyzed for synchronous and asynchronous hopping under nonfading and Rayleigh fading channels using the derived GAs. Results show that the maximum achievable normalized throughput is significantly larger than that obtainable with traditional MFSK. This is mainly due to the suppression of the MAI through DS processing *without* requiring additional bandwidth. The performance of the proposed networks is also compared to those based on MC-OOK and hybrid DS-MFSK.

For PN-MWSK, signal orthogonality is achieved in the time domain, as opposed to the frequency domain for MFSK. Hence, it is expected that the sensitivity to hop timing error increases with M, and the sensitivity to hop frequency error decreases with M. Hop timing error not only results in a decrease in the received symbol energy, but also generates additional self-interference due to the breakdown of orthogonality among the PN-MWSK signals. We assume the Tikhonov distribution [12] for the hop timing error and derive a GA for the additional self-interference term. Results show that the sensitivity to hop timing error increases with M as expected, resulting in an optimum value of M maximizing the maximum achievable normalized throughput. This contrasts with the case of perfect hop timing synchronization, where the throughput increases with increasing M for both nonfading and Rayleigh fading channels.[1]

The remainder of this paper is organized as follows. System and channel models are presented in Section II, and in Section III, the decision variables and GAs for the MAI are derived. In Section IV, the effect of imperfect hop timing synchronization is analyzed, and in Section V, numerical results are presented. Finally, conclusions are drawn in Section VI.

II. System and Channel Model

The system considered in this paper is a homogeneous FHSS-MA network with K identical active users (transmitter–receiver pairs), as described in [1]. The distinction is the fact that PN-MWSK is employed in place of MFSK. A block diagram of the proposed system is shown in Fig. 1. With PN-MWSK, $\log_2 M$ binary information bits are grouped to choose one of the M Walsh sequences of length M. The Walsh sequence is then overlaid by a user-specific complex PN sequence with chip rate identical to that of the Walsh sequence. The transmitters send one PN-MWSK symbol per hop (fast hopping) in one of the q available frequency-hop slots, and each user employs a Markov hopping pattern [13]. We do not put any constraint on the frequency separation between contiguous frequency-hop slots (slot frequency separation) for asynchronous hopping networks. For synchronous hopping networks, the

[1]The analysis, of course, is valid only for values of M up to the point where the flat-fading assumption within a hop holds.

slot frequency separation is assumed to be M/T_s to maintain orthogonality. The baseband-equivalent transmitted waveform of the kth user transmitting symbol $m_k \in \{1, \ldots, M\}$ during a symbol (hop) duration $[0, T_s)$ can be represented as

$$p_k^{m_k}(t) = \sum_{n=0}^{M-1} w_n^{m_k} \left(a_{k,n}^I + j a_{k,n}^Q \right) h_c(t - nT_c). \quad (1)$$

Here, $\{w_n^{m_k}\}_{n=0}^{M-1}$ is the Walsh sequence of length M corresponding to symbol m_k taking on the values of $+1$ and -1. Also, $\{a_{k,n}^I\}$ and $\{a_{k,n}^Q\}$ are the in-phase and quadrature-phase PN sequences for the kth user, where $a_{k,n}^I$ and $a_{k,n}^Q$ are assumed to be independent and identically distributed (i.i.d.) and equally likely to be $+1/\sqrt{2}$ or $-1/\sqrt{2}$. The chip pulse shape $h_c(t)$ equals 1 for $0 \le t \le T_c$ and zero otherwise, where $T_c = T_s/M$ is the chip duration.

Let f_0 be the hop carrier frequency used by the reference user (say user number zero) during the hop duration $[0, T_s)$. Also, let K' be the number of interfering users using a hop carrier frequency in the set $\mathcal{F} \triangleq \{f_{-S}, \ldots, f_{-1}, f_0, f_1, \ldots, f_S\}$, where S is the number of neighboring frequency-hop slots on each side of the dehopped slot taken into account. We assume that the hopping pattern of a receiver is perfectly synchronized to that of the corresponding transmitter. Then, the complex baseband-equivalent signal at the receiver of the reference user during the hop duration can be written as

$$r(t) = \sqrt{\frac{E_{s,0}}{T_s}} p_0^{m_0}(t) e^{j\theta_0} + \sum_{k=1}^{K'} \sqrt{\frac{E_{s,k}}{T_s}} p_k^{m_k}(t - \tau_k) e^{j(2\pi \Delta f_k t + \theta_k)} + z(t) \quad (2)$$

where θ_0 is the random phase offset of the reference user's signal uniformly distributed on $[0, 2\pi)$. The terms $\tau_k \in (-T_s, T_s)$ and $\theta_k \in [0, 2\pi)$ are the uniform random delay and phase of the kth interfering user's signal, respectively, and Δf_k is the hop carrier frequency difference between the reference user's signal and the kth interfering user's signal. Also, $z(t)$ is the equivalent low-pass complex white Gaussian noise process with two-sided power spectral density N_0 and $E_{s,k}$ is the received symbol energy of the kth interfering user. Assuming perfect power control, $E_{s,k}$ has a constant value of E_s ($= E_b \log_2 M$, where E_b is the received energy per bit) without fading. Under the independent Rayleigh fading assumption, $E_{s,k}$ is assumed to be i.i.d. and exponentially distributed with probability density function (pdf) $p_{E_{s,k}}(x) = (1/E_s) e^{-x/E_s}, x \ge 0$, and independent between hops. This fading model is widely adopted as a first-order approximation to actual physical channels [1], [8]–[11].

After observing $r(t)$ in $[0, T_s)$, the receiver computes the M decision variables $|U_l|,\ l = 1, \ldots, M$, given as

$$|U_l| = \left| \frac{1}{\sqrt{T_s}} \int_0^{T_s} r(t) p_0^l(t)^* dt \right|, \quad l = 1, \ldots, M \quad (3)$$

where x^* denotes the complex conjugate of x. Then, the index of the largest decision variable is chosen as the estimate $\hat{m}_0$ of the transmitted symbol.

III. Gaussian Approximations

In order to derive the GAs, we first derive the expressions for the U_l's. We consider the asynchronous hopping case, and the results for the synchronous hopping case may be obtained from the asynchronous hopping case by setting $\tau_k = 0$ for all k. By inserting (2) into (3), it is straightforward to show that the U_l's may be written as

$$U_l = U_l^s + \sum_{k=1}^{K'} U_{l,k}^{\mathrm{MAI}} + z_l, \quad l = 1, \ldots, M. \quad (4)$$

Here, z_l's are i.i.d. zero-mean complex Gaussian random variables with independent real and imaginary parts with identical variance $N_0/2$, $U_l^s \triangleq \sqrt{E_{s,0}} e^{j\theta_0} \delta_{m_0,l}$ and

$$U_{l,k}^{\mathrm{MAI}} \triangleq \frac{\sqrt{E_{s,k}}}{T_s} \int_0^{T_s} p_k^{m_k}(t - \tau_k) e^{j(2\pi \Delta f_k t + \theta_k)} p_0^l(t)^* dt. \quad (5)$$

The term $U_{l,k}^{\mathrm{MAI}}$ can be evaluated by separately considering the cases for $0 \le \tau_k < T_s$ and $-T_s \le \tau_k < 0$. In the Appendix, $U_{l,k}^{\mathrm{MAI}}$ is shown to be

$$U_{l,k}^{\mathrm{MAI}} = \frac{\sqrt{E_{s,k}}}{M} e^{j(\pi\rho_k(2L_k + \mu_k + 1) + \theta_k)} \cdot \left\{ \left[\frac{\sin(\pi\rho_k(1 - \mu_k))}{\pi\rho_k} \cdot \sum_{n=0}^{M-L_k-1} \left(c_{0,n+L_k}^l\right)^* c_{k,n}^{m_k} e^{j(2\pi\rho_k n)} \right] + \left[\frac{\sin(\pi\rho_k\mu_k)}{\pi\rho_k} \cdot \sum_{n=0}^{M-L_k-2} \left(c_{0,n+L_k+1}^l\right)^* c_{k,n}^{m_k} e^{j(2\pi\rho_k(n+(1/2)))} \right] \right\} \quad (6)$$

for the case when $0 \le \tau_k < T_s$. Here, $\rho_k \triangleq \Delta f_k T_c$ is the normalized hop carrier frequency difference between the reference user's signal and the kth interfering user's signal. The nonnegative integer term L_k and $0 \le \mu_k < 1$ satisfy $|\tau_k| = (L_k + \mu_k) T_c$, and $c_{k,n}^{m_k} = w_n^{m_k}(a_{k,n}^I + j a_{k,n}^Q)$. For the case when $-T_s \le \tau_k < 0$, $U_{l,k}^{\mathrm{MAI}}$ are given by (6) with $\left(c_{0,n+L_k}^l\right)^*$, $\left(c_{0,n+L_k+1}^l\right)^*$ and $c_{k,n}^{m_k}$ replaced with $c_{k,n+L_k}^{m_k}$, $c_{k,n+L_k+1}^{m_k}$, and $\left(c_{0,n}^l\right)^* e^{-j(2\pi\rho_k(L_k+\mu_k))}$, respectively.

A. Gaussian Approximation 1 (GA1)

Applying the GA to the MAI term is widely employed and accepted in the analysis of systems with some form of DS processing gain [14], [15]. An example similar to the system model adopted in this paper is given in [16], which was later adopted in analyzing the conditional error probability for FHSS-MA networks employing noncoherent hybrid DS-MFSK [5]. We expect that the DS processing gain inherent in PN-MWSK justifies our use of the GA for MAI, which is confirmed in Section V.

Based on the GA, in order to evaluate the conditional symbol error probability, we first approximate the MAI terms $U_{l,k}^{\mathrm{MAI}}$, $k = 1, \ldots, K'$ as Gaussian random variables. For asynchronous

hopping, $U_{l,k}^{\mathrm{MAI}}$ is easily shown from (6) to have zero mean and variance conditioned on ρ_k given as

$$\begin{aligned}\mathrm{E}_{\{\tau_k,c_{k,n}^{m_k},E_{s,k}\}}&\left\{\left|U_{l,k}^{\mathrm{MAI}}\right|^2\middle|\rho_k\right\}\\ =&\frac{E_s}{M^2}\left[\mathrm{E}_{\mu_k}\left\{\frac{\sin^2(\pi\rho_k(1-\mu_k))}{(\pi\rho_k)^2}\right\}\right.\\ &\cdot\mathrm{E}_{L_k}\left\{\sum_{n=0}^{M-L_k-1}\left|c_{0,n+L_k}^{l}\right|^2\left|c_{k,n}^{m_k}\right|^2\right\}\\ &+\mathrm{E}_{\mu_k}\left\{\frac{\sin^2(\pi\rho_k\mu_k)}{(\pi\rho_k)^2}\right\}\\ &\left.\cdot\mathrm{E}_{L_k}\left\{\sum_{n=0}^{M-L_k-2}\left|c_{0,n+1+L_k}^{l}\right|^2\left|c_{k,n}^{m_k}\right|^2\right\}\right]\\ =&\frac{E_s}{3M}\Lambda(\rho_k)\end{aligned}\tag{7}$$

for both nonfading and Rayleigh fading cases with

$$\Lambda(x)\triangleq\frac{6}{(2\pi x)^2}\left[1-\frac{\sin(2\pi x)}{2\pi x}\right].\tag{8}$$

Then, the variance of the second term in (4) (the aggregate MAI) denoted $\beta(K')$ is obtained as

$$\beta(K')\triangleq\frac{E_s}{3M}\sum_{k=1}^{K'}\mathrm{E}_{\rho_k}\{\Lambda(\rho_k)\}\tag{9}$$

$$=\frac{K'E_s}{3M}\frac{1}{1+2S}\left[1+\sum_{\substack{i=-S\\ i\neq 0}}^{S}\Lambda((f_0-f_i)T_c)\right].\tag{10}$$

Note that as with conventional DS spread-spectrum multiple-access networks [17], [18], the variance of the aggregate MAI, $\beta(K')$, bears a division by a factor of M, representing the DS processing gain. This DS processing gain accounts for the drastic performance improvement compared with traditional MFSK.

For synchronous hopping networks with slot frequency separation M/T_s, signals present in neighboring frequency-hop slots are orthogonal to the reference user's signal and thus, do not act as interference. Hence, for synchronous hopping, $\beta(K')$ reduces to

$$\beta(K')=\frac{K'E_s}{M}\tag{11}$$

for both nonfading and Rayleigh fading channels.

For nonfading channels, we may now approximate the U_l's as i.i.d. complex Gaussian random variables as follows:

$$U_{m_0}\sim N\left(\sqrt{E_s}e^{j\theta_0},\beta(K')+N_0\right)\tag{12}$$

$$U_l\sim N(0,\beta(K')+N_0),\quad l\neq m_0.\tag{13}$$

Thus, the conditional symbol-error probability given K' interfering users can be approximated as [19]

$$P_s(K')=\sum_{n=1}^{M-1}\binom{M-1}{n}\frac{(-1)^{(n+1)}}{n+1}\cdot\exp\left[-\frac{n}{(n+1)\beta'(K')}\right]\tag{14}$$

where

$$\beta'(K')\triangleq\left(\frac{E_s}{\beta(K')+N_0}\right)^{-1}\tag{15}$$

is the inverse of the equivalent SNR at the matched-filter output.

For Rayleigh fading channels, the reference user's signal contributes to the variance of U_{m_0}, and we may approximate U_l's as

$$U_{m_0}\sim N(0,E_s+\beta(K')+N_0)\tag{16}$$

$$U_l\sim N(0,\beta(K')+N_0),\quad l\neq m_0.\tag{17}$$

The conditional symbol-error probability is then approximated as [19]

$$P_s(K')=\sum_{n=1}^{M-1}\binom{M-1}{n}\frac{(-1)^{n+1}}{n+1+n\beta'(K')}.\tag{18}$$

The merit of GA1 is that it results in simple closed-form expressions for $P_s(K')$. The average error probability with K active users is then given as [3]

$$P_a(K)=\sum_{K'=0}^{K-1}\binom{K-1}{K'}p_h^{K'}(1-p_h)^{K-1-K'}P_s(K')\tag{19}$$

where p_h is the probability that an interfering user uses a hop carrier frequency in the set $\mathcal{F}$. For q sufficiently larger than $2S$, the probability of an interfering user hopping into the carrier set $\mathcal{F}$ for two consecutive hops can safely be neglected. Furthermore, the edge effect, i.e., the probability of the reference user hopping to a frequency-hop slot near the edge of the RF band, where the number of available neighboring frequency-hop slots on one side is less than S, may also be neglected for sufficiently large q. Hence, we may approximate p_h as follows given that the above two conditions are met:

$$p_h\approx\frac{2(1+2S)}{q}.\tag{20}$$

As will be seen in Section V, values of $P_s(K')$, $K'\geq 1$, for many system configurations lies above 0.1, in which case simple GA1 suffices. However, for some cases, e.g., with large M and no fading under asynchronous hopping, the accuracy of GA1 degrades for small values of $P_s(K')$. Therefore, we consider a more accurate (but not as easily computed) approximation to $P_s(K')$ in the next section.

B. Gaussian Approximation 2 (GA2)

For the case of nonfading channels, unlike GA1, we use the variance of $U_{l,k}^{\mathrm{MAI}}$ conditioned on τ_k and ρ_k to first compute the conditional error probability $P_s(K'|\bar{\tau},\bar{\rho})$ with $\bar{\tau}\triangleq(\tau_1,\ldots,\tau_{K'})$ and $\bar{\rho}\triangleq(\rho_1,\ldots,\rho_{K'})$. The conditional error probability $P_s(K'|\bar{\tau},\bar{\rho})$ is then averaged over $\bar{\tau}$ and $\bar{\rho}$ to give a second approximation to $P_s(K')$, denoted GA2. The variance of $U_{l,k}^{\mathrm{MAI}}$ conditioned on τ_k and ρ_k can be computed from (6) as

$$\begin{aligned}\mathrm{E}_{c_{k,n}^{m_k}}&\left\{\left|U_{l,k}^{\mathrm{MAI}}\right|^2\middle|\tau_k,\rho_k\right\}\\ =&\frac{E_s}{M^2}\left[\frac{\sin^2(\pi\rho_k(1-\mu_k))}{(\pi\rho_k)^2}(M-L_k)\right.\\ &\left.+\frac{\sin^2(\pi\rho_k\mu_k)}{(\pi\rho_k)^2}(M-L_k-1)\right].\end{aligned}\tag{21}$$

Thus, U_l's conditioned on $\bar{\tau}$ and $\bar{\rho}$ are approximated as

$$U_{m_0}|_{\{\bar{\tau},\bar{\rho}\}} \sim N\left(\sqrt{E_s}e^{j\theta_0}, \beta\left(K'|\,\bar{\tau},\bar{\rho}\right)+N_0\right) \quad (22)$$

$$U_l|_{\{\bar{\tau},\bar{\rho}\}} \sim N\left(0, \beta\left(K'|\,\bar{\tau},\bar{\rho}\right)+N_0\right), \quad l \neq m_0 \quad (23)$$

where

$$\begin{aligned}\beta\left(K'|\,\bar{\tau},\bar{\rho}\right) &\triangleq \sum_{k=1}^{K'} \mathrm{E}_{c_{k,n}^{m_k}}\left\{\left|U_{l,k}^{\mathrm{MAI}}\right|^2 \middle| \tau_k,\rho_k\right\} \\ &= \sum_{k=1}^{K'} \frac{E_s}{M^2}\left[\frac{\sin^2(\pi\rho_k(1-\mu_k))}{(\pi\rho_k)^2}(M-L_k)\right. \\ &\quad \left.+\frac{\sin^2(\pi\rho_k\mu_k)}{(\pi\rho_k)^2}(M-L_k-1)\right]. \end{aligned} \quad (24)$$

The conditional error probability $P_s(K'|\bar{\tau},\bar{\rho})$ is then given by (14) with $\beta'(K')$ replaced with $\beta'\left(K'|\,\bar{\tau},\bar{\rho}\right)$, which is in turn given by (15) with $\beta(K')$ replaced with $\beta\left(K'|\,\bar{\tau},\bar{\rho}\right)$. Averaging $P_s(K'|\bar{\tau},\bar{\rho})$ over $\bar{\tau}$ and $\bar{\rho}$, we have

$$\begin{aligned}P_s(K') = &\sum_{n=1}^{M-1}\binom{M-1}{n}\frac{(-1)^{(n+1)}}{n+1} \\ &\cdot\mathrm{E}_{\{\bar{\tau},\bar{\rho}\}}\left\{\exp\left[-\frac{n}{(n+1)\beta'\left(K'|\bar{\tau},\bar{\rho}\right)}\right]\right\}. \end{aligned} \quad (25)$$

Using the fact that τ_k's and ρ_k's are i.i.d., the expectation in (25) may be relatively easily evaluated via the Monte–Carlo method [20].

This is much simpler than straightforward system simulation based on directly generating the decision variables given by (4), mainly due to two reasons. One is that the computational complexity of the argument of the expectation in (25) does not depend on M, whereas the complexity of generating the decision variables based on (4) and (6) increases as M^2. Another reason is that the number of required Monte–Carlo iterations for computing the expectation in (25) does not depend on the value $P_s(K')$ being estimated. On the other hand, the number of required Monte–Carlo iterations for the decision variable-based method increases with decreasing $P_s(K')$. We compared the approximate computation time requirements for the two methods and have concluded that estimating $P_s(K')$ via (25) (GA2) is drastically simpler. For example, with $M=16$, $K'=3$, $E_b/N_0=30$ dB, and $S=3$ for which $P_s(K')\simeq 1.2\times10^{-4}$, the required simulation time for the decision variable-based method was approximately 700 times that based on GA2. Moreover, for $M=64$, $K'=25$, $E_b/N_0=30$ dB, and $S=3$ for which $P_s(K')\simeq 1.3\times10^{-4}$, the required simulation time for the decision variable-based method was approximately 8000 times that based on GA2. For the above results, we observed 1000 error samples for the decision variable-based simulation and performed 10 000 Monte–Carlo iterations for GA2.

For the case of Rayleigh fading, we further condition the variance of $U_{l,k}^{\mathrm{MAI}}$ on $E_{s,k}$. Then, the variance of $U_{l,k}^{\mathrm{MAI}}$ conditioned on $E_{s,k}$, τ_k, and ρ_k is given by (21) with E_s replaced with $E_{s,k}$. This results in the following GA for U_l's conditioned on $\bar{E}_s \triangleq (E_{s,1},\ldots,E_{s,K'})$, $\bar{\tau}$, and $\bar{\rho}$:

$$U_{m_0}|_{\{\bar{E}_s,\bar{\tau},\bar{\rho}\}} \sim N\left(0, E_s+\beta\left(K'|\,\bar{E}_s,\bar{\tau},\bar{\rho}\right)+N_0\right) \quad (26)$$

$$U_l|_{\{\bar{E}_s,\bar{\tau},\bar{\rho}\}} \sim N\left(0, \beta\left(K'|\,\bar{E}_s,\bar{\tau},\bar{\rho}\right)+N_0\right), \quad l \neq m_0 \quad (27)$$

where $\beta\left(K'|\,\bar{E}_s,\bar{\tau},\bar{\rho}\right)$ is given by (24) with E_s replaced with $E_{s,k}$. The conditional error probability $P_s(K')$ is then given by

$$\begin{aligned}P_s(K') = &\sum_{n=1}^{M-1}\binom{M-1}{n} \\ &\mathrm{E}_{\{\bar{E}_s,\bar{\tau},\bar{\rho}\}}\left\{\frac{(-1)^{n+1}}{n+1+n\beta'\left(K'|\,\bar{E}_s,\bar{\tau},\bar{\rho}\right)}\right\} \end{aligned} \quad (28)$$

where $\beta'\left(K'|\,\bar{E}_s,\bar{\tau},\bar{\rho}\right)$ is given by (15) with $\beta(K')$ replaced with $\beta\left(K'|\,\bar{E}_s,\bar{\tau},\bar{\rho}\right)$. The expectation in (28) may again be relatively easily evaluated via the Monte–Carlo method.

IV. Effect of Imperfect Hop Timing Synchronization

Results presented in Section III assume perfect hop synchronization in the sense that the receiver has perfect knowledge of the hop timing of the target transmitter. In practice, such ideal conditions are seldom met, and the accuracy with which the synchronization can be accomplished affects network performance. Since the chip duration $T_c=(\log_2(M)/M)T_b$ decreases with increasing M for a fixed bit duration T_b for PN-MWSK, the sensitivity to hop timing error increases with M. On the other hand, since the frequency-hop slot bandwidth is inversely proportional to T_c, the sensitivity to hop frequency error will decrease with increasing M. In this section, we analyze the effect of imperfect hop timing synchronization on the error probability with perfect hop frequency synchronization for asynchronous hopping networks.

We assume that the reference user's received signal has a hop timing error τ_0 which follows the Tikhonov distribution [12]. Defining the normalized hop timing error as $\lambda \triangleq \tau_0/T_b$, the pdf of λ is given by

$$f(\lambda)=\frac{1}{2\lambda_{\max}}\frac{\exp\left[\left(\frac{\lambda_{\max}}{\pi\sigma_\lambda}\right)^2\cos\left(\frac{\pi\lambda}{\lambda_{\max}}\right)\right]}{I_0\left[\left(\frac{\lambda_{\max}}{\pi\sigma_\lambda}\right)^2\right]}, \quad |\lambda|\le\lambda_{\max}. \quad (29)$$

Here, $I_0(x)$ is the modified Bessel function of order zero, σ_λ^2 is the variance of λ, and $\lambda_{\max}$ is the maximum absolute normalized hop timing error.

In the presence of a hop timing error of τ_0 which is assumed to satisfy $|\tau_0|<T_c$, the effect of the reference user's signal on the lth matched-filter output is given by

$$U_l^s=\frac{\sqrt{E_{s,0}}}{T_s}\int_0^{T_s} p_0^{m_0}(t-\tau_0)e^{j\theta_0}p_0^l(t)^*\,dt. \quad (30)$$

This expression is identical to that for $U_{l,k}^{\mathrm{MAI}}$ given by (5) with $k=0$ and $\Delta f_k=0$. Hence, it is straightforward using (6) to see that U_l^s with hop timing error $0\le\tau_0<T_c$ is given by

$$U_l^s=\frac{\sqrt{E_{s,0}}}{M}e^{j\theta_0}\left[(1-\mu_0)M\delta_{m_0,l}+\mu_0\sum_{n=0}^{M-2}(c_{0,n+1}^l)^*c_{0,n}^{m_0}\right] \quad (31)$$

where $\mu_0\triangleq|\tau_0|/T_c$. For the case when $-T_c<\tau_0<0$, U_l^s is given by (31), with $(c_{0,n+1}^l)^*$ and $c_{0,n}^{m_0}$ replaced with $c_{0,n+1}^{m_0}$

and $(c_{0,n}^{l})^*$, respectively. On the other hand, $U_{l,k}^{\mathrm{MAI}}$ in (4) is unaffected by hop timing error for asynchronous hopping.

For nonfading channels, it is easily shown from (31) that the mean and variance of U_l^s conditioned on μ_0 are given as

$$\mathrm{E}_{c_{0,n}^{m_0}}\left\{U_l^s|\,\mu_0\right\}=\begin{cases}\sqrt{E_s}e^{j\theta_0}\,(1-\mu_0)\,, & \text{for } l=m_0\\ 0, & \text{otherwise}\end{cases} \tag{32}$$

and

$$\begin{aligned}\beta_s(\mu_0)&\triangleq\mathrm{E}_{c_{0,n}^{m_0}}\left\{\left|U_l^s-\mathrm{E}_{c_{0,n}^{m_0}}\left\{U_l^s|\,\mu_0\right\}\right|^2\middle|\,\mu_0\right\}\\&=\frac{E_s}{M}\left(1-\frac{1}{M}\right)\mu_0^2.\end{aligned} \tag{33}$$

This implies that the hop timing error results in an effective decrease in the received symbol energy and an effective increase in self-interference. Since U_l^s and $U_{l,k}^{\mathrm{MAI}}$ are statistically independent, GA1 for the U_l's given μ_0 is obtained from (12), (13), (32), and (33) as

$$U_{m_0}\sim N\left(\sqrt{E_s}e^{j\theta_0}\,(1-\mu_0)\,,\beta_s(\mu_0)+\beta(K')+N_0\right) \tag{34}$$

$$U_l\sim N\left(0,\beta_s(\mu_0)+\beta(K')+N_0\right),\quad l\neq m_0. \tag{35}$$

Similarly, GA2 for the U_l's given μ_0 is obtained from (22), (23), (32), and (33) as

$$\begin{aligned}U_{m_0}|_{\{\bar\tau,\bar\rho\}}\sim&N\left(\sqrt{E_s}e^{j\theta_0}(1-\mu_0),\beta_s(\mu_0)\right.\\&\left.+\beta\left(K'\,|\bar\tau,\bar\rho\right)+N_0\right)\end{aligned} \tag{36}$$

$$\begin{aligned}U_l|_{\{\bar\tau,\bar\rho\}}\sim&N\left(0,\beta_s(\mu_0)+\beta\left(K'\,|\bar\tau,\bar\rho\right)+N_0\right),\\&l\neq m_0.\end{aligned} \tag{37}$$

The conditional symbol error probability $P_s(K'|\mu_0)$ for GA1 and GA2 are then given by (14) and (25), respectively, with $\beta'(K')$ replaced with

$$\beta'(K')=\begin{cases}\left(\frac{D^2(\mu_0)}{\beta_s(\mu_0)+\beta(K')+N_0}\right)^{-1}, & \text{for GA1}\\ \left(\frac{D^2(\mu_0)}{\beta_s(\mu_0)+\beta(K'|\bar\tau,\bar\rho)+N_0}\right)^{-1}, & \text{for GA2}\end{cases} \tag{38}$$

where

$$D(\mu_0)\triangleq\sqrt{E_s}\,(1-\mu_0)\,. \tag{39}$$

Due to difficulties in analytically averaging $P_s(K'|\mu_0)$ over μ_0, we approximate $P_s(K')$ by (14) and (25) for GA1 and GA2, respectively, by replacing $D(\mu_0)$ and $\beta_s(\mu_0)$ in (38) with their respective averaged values over $\mu_0(=(M/\log_2 M)|\lambda|)$, given by

$$\begin{aligned}D_{\mathrm{avg}}&\triangleq\int_{-\lambda_{\max}}^{\lambda_{\max}}D(\mu_0)f(\lambda)d\lambda\\&=\frac{\sqrt{E_s}}{\lambda_{\max}I_0\left[\left(\frac{\lambda_{\max}}{\pi\sigma_\lambda}\right)^2\right]}\int_0^{\lambda_{\max}}\left(1-\frac{M}{\log_2 M}\lambda\right)\\&\quad\cdot\exp\left[\left(\frac{\lambda_{\max}}{\pi\sigma_\lambda}\right)^2\cos\left(\frac{\pi\lambda}{\lambda_{\max}}\right)\right]d\lambda\end{aligned} \tag{40}$$

and

$$\begin{aligned}\beta_{s,\mathrm{avg}}&\triangleq\int_{-\lambda_{\max}}^{\lambda_{\max}}\beta_s(\mu_0)f(\lambda)d\lambda\\&=\frac{E_s(M-1)}{(\log_2 M)^2}\frac{1}{\lambda_{\max}I_0\left[\left(\frac{\lambda_{\max}}{\pi\sigma_\lambda}\right)^2\right]}\int_0^{\lambda_{\max}}\lambda^2\\&\quad\cdot\exp\left[\left(\frac{\lambda_{\max}}{\pi\sigma_\lambda}\right)^2\cos\left(\frac{\pi\lambda}{\lambda_{\max}}\right)\right]d\lambda.\end{aligned} \tag{41}$$

For Rayleigh fading channels, it is readily seen that U_l's for GA1 are given by

$$U_{m_0}\sim N\left(0,E_s\,(1-\mu_0)^2+\beta_s(\mu_0)+\beta(K')+N_0\right) \tag{42}$$

$$U_l\sim N\left(0,\beta_s(\mu_0)+\beta(K')+N_0\right),\quad l\neq m_0. \tag{43}$$

As for GA2, which uses the conditional variance of the aggregate MAI, $\beta\left(K'\left|\bar E_s,\bar\tau,\bar\rho\right.\right)$, U_l's conditioned on $\bar E_s$, $\bar\tau$ and $\bar\rho$ can be written as

$$\begin{aligned}U_{m_0}|_{\{\bar E_s,\bar\tau,\bar\rho\}}\sim&N\left(0,E_s(1-\mu_0)^2+\beta_s(\mu_0)\right.\\&\left.+\beta\left(K'\left|\bar E_s,\bar\tau,\bar\rho\right.\right)+N_0\right)\end{aligned} \tag{44}$$

$$\begin{aligned}U_l|_{\{\bar E_s,\bar\tau,\bar\rho\}}\sim&N\left(0,\beta_s(\mu_0)+\beta\left(K'\left|\bar E_s,\bar\tau,\bar\rho\right.\right)+N_0\right),\\&l\neq m_0.\end{aligned} \tag{45}$$

Then, $P_s(K')$ is evaluated using (18) and (28) for GA1 and GA2, respectively, using $\beta'(K')$ given in (38), with $D(\mu_0)$ and $\beta_s(\mu_0)$ replaced with D_{avg} and $\beta_{s,\mathrm{avg}}$, respectively, and $\beta\left(K'\left|\bar\tau,\bar\rho\right.\right)$ replaced with $\beta\left(K'\left|\bar E_s,\bar\tau,\bar\rho\right.\right)$.

V. Numerical Results

For all the numerical results presented in this section, E_b/N_0 is assumed to be 30 dB and the frequency separation between contiguous frequency-hop slots to be M/T_s. Note that MAI from the dehopped slot and three contiguous neighboring slots on each side of the dehopped slot ($S=3$) are considered for asynchronous networks employing PN-MWSK. It was verified via simulations that interference from frequency-hop slots further away may safely be neglected.

In Figs. 2 and 3, $P_s(K')$ predicted by GA1 and GA2 are compared with those obtained via simulations for asynchronous networks employing PN-MWSK. Fig. 2 indicates that for nonfading channels, GA2 accurately predicts the simulation results for all cases considered. The simpler GA1 accurately predicts $P_s(K')$ for $P_s(K')>0.1$, but gives optimistic results for $P_s(K')<0.1$. Therefore, for subsequent analyses for nonfading channels, GA2 is used for $P_s(K')<0.1$ and GA1 is used for $P_s(K')\geq 0.1$. For Rayleigh fading channels, we observe that GA1 and GA2 both fit the simulation results quite well. We believe that the improved accuracy of GA1 for smaller values of $P_s(K')$ under Rayleigh fading is due to the additional randomness introduced by the random fading amplitudes. Hence, we adopt the simpler GA1 for networks under Rayleigh fading. For synchronous hopping networks, GA1 may safely be used for all cases of interest, with and without fading, as shown in Figs. 4 and 5.

The maximum of the normalized network throughput $w(K)$ is defined below, denoted $w_{\max}\triangleq\max_K w(K)$, assuming bi-

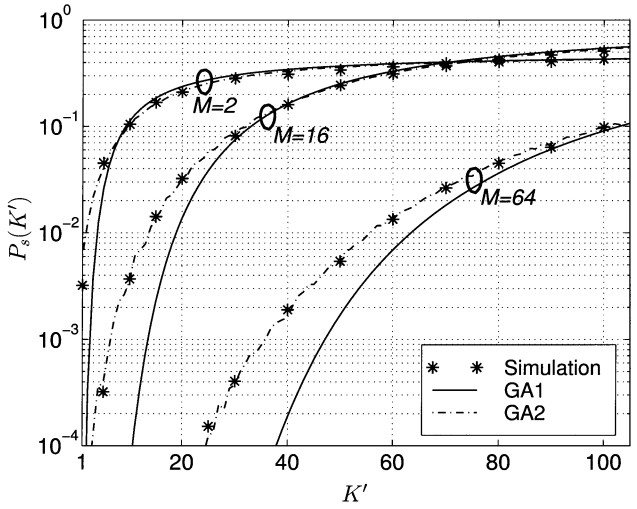

Fig. 2. Comparison of $P_s(K')$ obtained via GA1 and GA2 with simulation results for asynchronous networks employing PN-MWSK without fading.

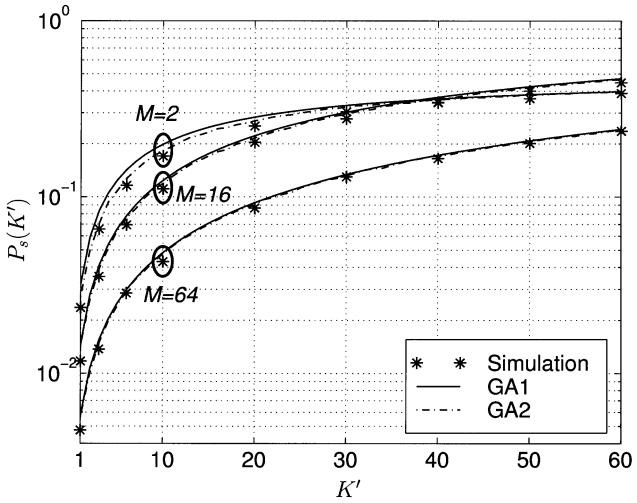

Fig. 3. Comparison of $P_s(K')$ obtained via GA1 and GA2 with simulation results for asynchronous networks employing PN-MWSK under Rayleigh fading.

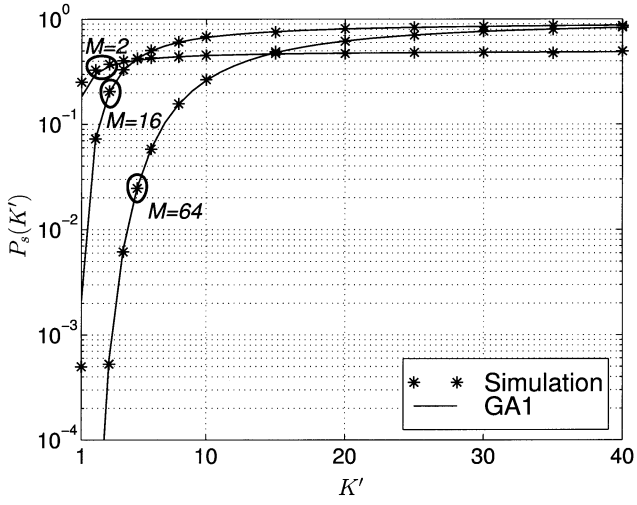

Fig. 4. Comparison of $P_s(K')$ obtained via GA1 with simulation results for synchronous networks employing PN-MWSK without fading.

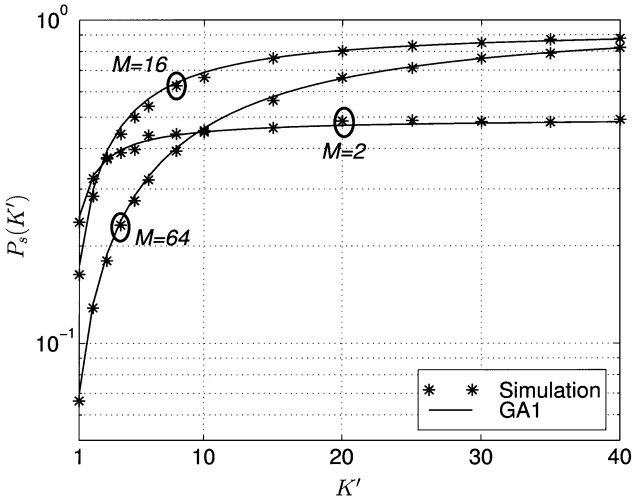

Fig. 5. Comparison of $P_s(K')$ obtained via GA1 with simulation results for synchronous networks employing PN-MWSK under Rayleigh fading.

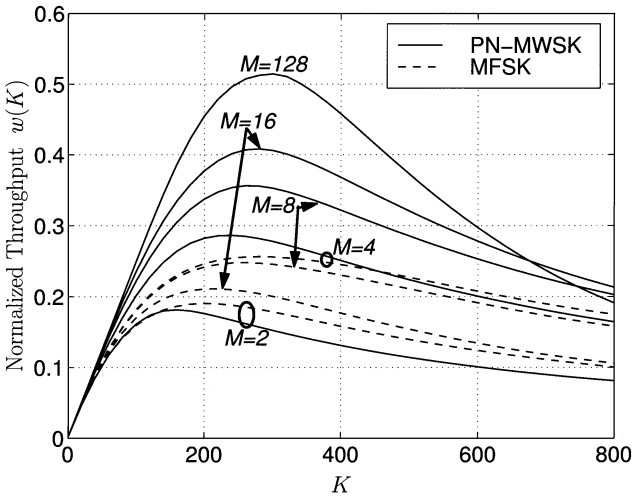

Fig. 6. Comparison of the normalized throughput for asynchronous networks employing PN-MWSK and MFSK without fading with $q_{M=2} = 200$.

nary codes achieving channel capacity is used as the performance measure [1], [3], [21]

$$w(K) = \frac{KC(K)}{W_{ss}T_b} = \frac{KC(K)}{2q_{M=2}} \tag{46}$$

where

$$C(K) = 1 + P_b(K)\log_2(P_b(K)) + (1 - P_b(K))\log_2(1 - P_b(K)) \tag{47}$$

is the channel capacity [19] with K active users in the network. Also, $P_b(K) = (M/2(M-1))P_a(K)$ is the average bit-error probability, W_{SS} is the total RF bandwidth allotted to the network, and $q_{M=2} = W_{SS}T_b/2$ is the number of available frequency-hop slots with $M = 2$. The total RF bandwidth W_{SS} and the data bit rate $1/T_b$ are assumed to be fixed, regardless of M, giving the number of available frequency-hop slots for a given M as $q_M = (2\log_2 M/M)q_{M=2}$. For the remainder of this section, we assume $q_{M=2} = 200$.

Figs. 6 and 7 show the normalized throughput versus the number of active users for nonfading and Rayleigh fading channels, respectively, for asynchronous networks employing

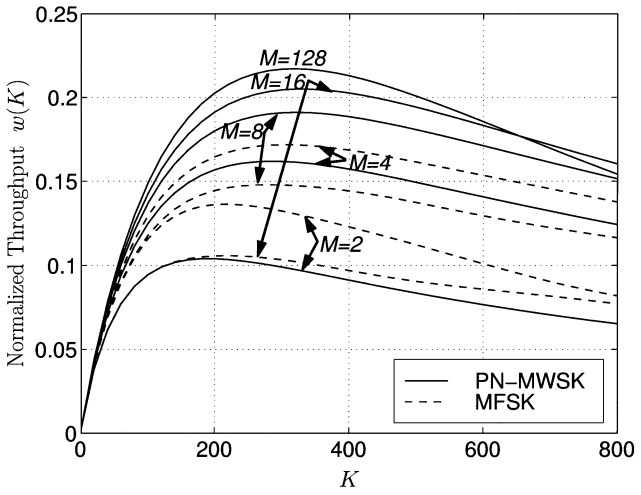

Fig. 7. Comparison of the normalized throughput for asynchronous networks employing PN-MWSK and MFSK under Rayleigh fading with $q_{M=2} = 200$.

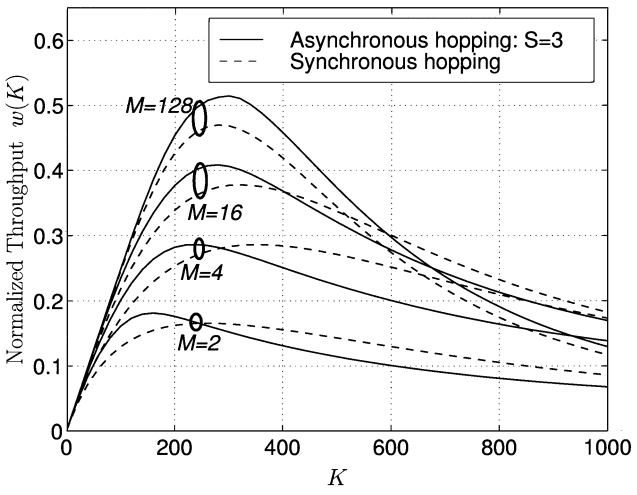

Fig. 8. Comparison of the normalized throughput for asynchronous and synchronous networks employing PN-MWSK without fading with $q_{M=2} = 200$.

PN-MWSK and MFSK.[2] First, in Fig. 6, we note that for networks employing PN-MWSK in nonfading channels, $w_{\max}$ increases with M for all values of M considered. This is because as M increases, the increase in MAI, due to the increase in the hit probability, is more than compensated by the combination of two factors. One is the DS processing gain and the other is the SNR gain, i.e., the decrease in required SNR in order to achieve a given BER with increasing M for M-ary orthogonal modulation under additive white Gaussian noise (AWGN) [19]. For networks employing PN-MWSK in Rayleigh fading channels, the increase in $w_{\max}$ with increasing M is much smaller compared with that of nonfading channels, as shown in Fig. 7. The reason for this is that the SNR gain due to M-ary orthogonal modulation is much smaller for Rayleigh fading channels [19].

Comparing the results for PN-MWSK and MFSK in Figs. 6 and 7, we observe that the proposed network employing PN-MWSK shows significantly improved throughput performance. For networks employing MFSK, $M = 4$ achieves the largest $w_{\max}$ for both nonfading and Rayleigh fading channels. In comparison, the proposed network with $M = 128$ gives approximately 100% and 25% larger $w_{\max}$ for nonfading and Rayleigh fading channels, respectively.[3]

It was shown in [1] that for networks employing MFSK, asynchronous networks outperform synchronous networks in terms of $w_{\max}$. In order to check if the same can be said for the PN-MWSK case, comparisons of asynchronous and synchronous networks employing PN-MWSK are shown in Figs. 8 and 9. For nonfading channels, asynchronous networks exhibit a slightly larger $w_{\max}$ than synchronous networks. For Rayleigh fading channels, synchronous networks obtain larger $w_{\max}$ than asynchronous networks for $M < 64$, while the trend is reversed for $M \geq 64$. Also note that the largest

[2]The results for MFSK were obtained from simulations with $S = 1$. It was verified that the interference from frequency-hop slots further away can safely be neglected.

[3]Although not shown in the paper, we have verified that for $M = 2, 4, \ldots, 128$, and $q_M \geq 20$, $w_{\max}$ obtained using the derived analytical results are in good agreement with simulation results and the edge effect can safely be neglected.

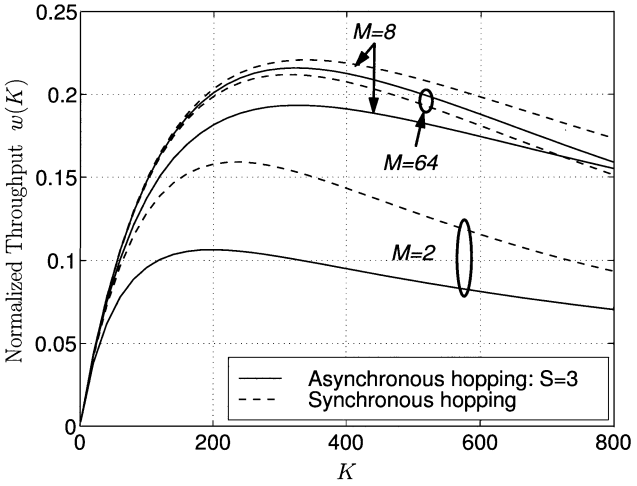

Fig. 9. Comparison of the normalized throughput for asynchronous and synchronous networks employing PN-MWSK under Rayleigh fading with $q_{M=2} = 200$.

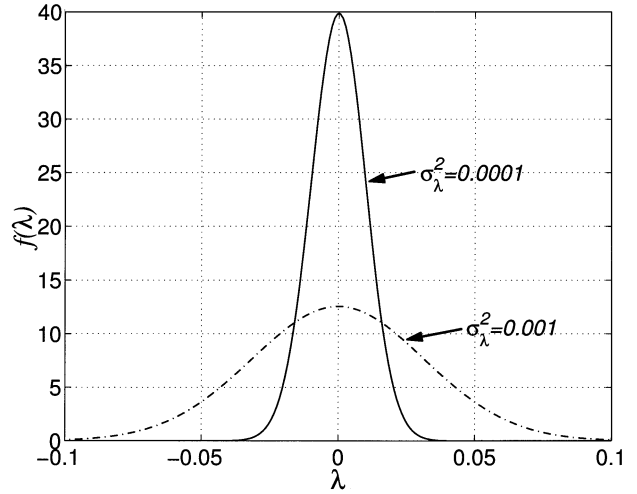

Fig. 10. Plots of the Tikhonov pdf $f(\lambda)$ for $\sigma_\lambda^2 = 0.0001$ and 0.001 with $\lambda_{\max} = 0.5$.

TABLE I
COMPARISON OF $K_{\max}$ SATISFYING $P_b \leq 10^{-2}$ FOR NETWORKS EMPLOYING PN-MWSK, MFSK, AND MC-OOK WITH $q_{M=2} = 200$

M	No fading						Rayleigh fading					
	PN-MWSK		MFSK		MC-OOK		PN-MWSK		MFSK		MC-OOK	
	Sync	Async	Sync	Async	Sync	Async	Sync	Async	Sync	Async	Sync	Async
2	10	22	5	27	18	32	8	6	4	8	14	4
4	20	50	5	36	18	32	10	9	4	9	14	4
8	48	83	4	35	18	31	11	10	4	8	14	4
16	76	116	3	31	18	31	11	11	3	6	14	4
32	106	147	2	26	18	31	11	12	1	4	14	4
64	137	173	1	22	18	31	11	12	1	3	14	4
128	165	195	1	18	18	31	11	12	1	2	14	4

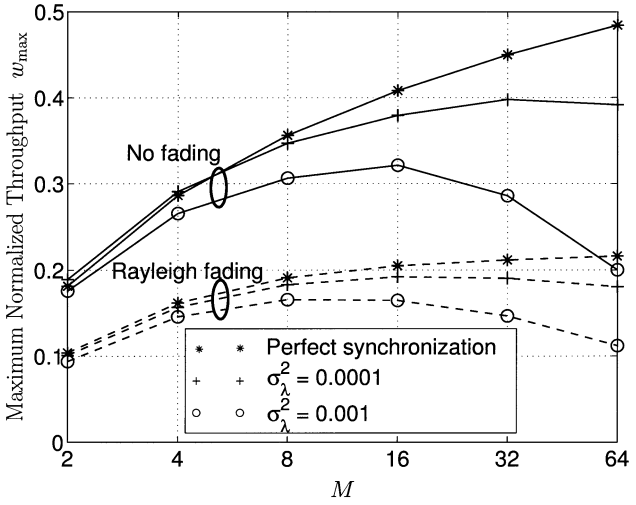

Fig. 11. Comparison of the maximum achievable normalized throughput for the cases of perfect and imperfect hop timing synchronizations for $\sigma_\lambda^2 = 0.0001$ and 0.001 with $\lambda_{\max} = 0.5$ and $q_{M=2} = 200$.

$w_{\max}$ is obtained with $M = 8$ for synchronous networks under Rayleigh fading.

Next, we consider the effect of imperfect hop timing synchronization on the performance of networks employing PN-MWSK with asynchronous hopping. Fig. 10 shows the Tikhonov pdfs of the normalized hop timing error $\lambda\ (= \tau_0/T_b)$ for $\sigma_\lambda^2 = 0.0001$ and 0.001 with $\lambda_{\max} = 0.5$. Since $\tau_0 = (M/\log_2(M))\lambda T_c$, $\lambda = 0.05$ in Fig. 10 corresponds to $\tau_0 = 0.1T_c$ and $0.53T_c$ for $M = 2$ and 64, respectively. In Fig. 11, $w_{\max}$ versus M is shown for the cases of perfect and imperfect hop timing synchronizations. As expected, for a given M under imperfect hop timing synchronization, $w_{\max}$ decreases with increasing σ_λ^2. This gives rise to the existence of an optimum value of M maximizing $w_{\max}$, unlike the case with perfect hop timing synchronization. Clearly, the sensitivity to hop timing error increases with increasing M due to a corresponding decrease in T_c for a fixed T_b.

In Table I, the maximum number of active users $K_{\max}$ satisfying $P_b \leq 10^{-2}$ are shown for networks employing PN-MWSK, MFSK, and MC-OOK. The results for MC-OOK were obtained via simulations using optimum decision thresholds. Observe that with asynchronous hopping, PN-MWSK with $M = 128$ gives approximately 440% and 35% larger $K_{\max}$ for nonfading and Rayleigh fading channels, respectively, compared with MFSK with $M = 4$. For networks employing MC-OOK, $K_{\max}$ clearly does not depend on M for synchronous hopping. Also, for asynchronous hopping, the dependence of $K_{\max}$ on M is minimal. We observe that for nonfading channels, PN-MWSK by far outperforms MC-OOK, whereas under Rayleigh fading MC-OOK slightly outperforms PN-MWSK.

Finally, in Table II, simulated values of $K_{\max}$ satisfying $P_b \leq 10^{-2}$ for hybrid DS-MFSK for $q = 20$ and $q = 1$ (corresponding to the no-hopping case) are compared with that of PN-MWSK. Asynchronous hopping is assumed with $S = 1$, and N denotes the DS processing gain per DS-MFSK symbol. For hybrid DS-MFSK without fading, it was shown in [5, Table IV] that $q = 1$ is optimum in terms of $K_{\max}$ for a large range of M. Hence, for nonfading channels, $M = 32$ with $q = 1$ ($N = 62$) achieves the largest $K_{\max}$ of 155 for hybrid DS-MFSK. On the other hand, Table II indicates that $K_{\max}$ for PN-MWSK increases with M and that PN-MWSK with $M \geq 64$ outperforms the optimum hybrid DS-MFSK. Before comparing the results for Rayleigh fading channels, we note that MFSK is a special case of hybrid DS-MFSK with $N = 1$. Hence, the results for MFSK given in Table I also need to be considered, and we find that MFSK with $M = 4$ gives the largest $K_{\max}$ of nine for hybrid DS-MFSK under Rayleigh fading. PN-MWSK achieves a larger $K_{\max}$ by using $M \geq 8$ for Rayleigh fading channels.

Now, we compare PN-MWSK with $M = 128$ and $q = 21$, with hybrid DS-MFSK with $q = 20$ with the optimum values $M = 8$ and $M = 4$ for nonfading and Rayleigh fading channels, respectively. Using similar values of q implies that the bandwidth occupied per frequency-hop slot is approximately the same. Observe that PN-MWSK with $M = 128$ gives approximately 85% and 50% larger $K_{\max}$ compared with the optimum hybrid DS-MFSK with $q = 20$ for nonfading

TABLE II
COMPARISON OF $K_{\max}$ SATISFYING $P_b \leq 10^{-2}$ FOR NETWORKS EMPLOYING PN-MWSK AND HYBRID DS-MFSK WITH $q_{M=2} = 200$ FOR ASYNCHRONOUS HOPPING

M	No fading						Rayleigh fading					
	PN-MWSK		Hybrid DS/MFSK ($q=20$)		Hybrid DS/MFSK ($q=1$)		PN-MWSK		Hybrid DS/MFSK ($q=20$)		Hybrid DS/MFSK ($q=1$)	
	q	$K_{\max}$	N	$K_{\max}$	N	$K_{\max}$	q	$K_{\max}$	N	$K_{\max}$	N	$K_{\max}$
2	200	22	10	55	200	67	200	6	10	6	200	6
4	200	50	10	90	200	108	200	9	10	8	200	8
8	150	83	8	106	150	129	150	10	8	7	150	7
16	100	116	5	97	100	148	100	11	5	5	100	5
32	62	147	3	66	62	155	62	12	3	4	62	4
64	37	173	2	41	37	154	37	12	2	2	37	2
128	21	195	1	18	21	141	21	12	1	2	21	1

and Rayleigh fading channels, respectively. Although we do not show the results, extensive simulation campaigns were performed, which verified that these observations are valid for a wide range of RF bandwidths (i.e., $q_{M=2}$) and also for the synchronous hopping case, as well. This improvement over hybrid DS-MFSK is mainly due to the fact that with PN-MWSK, the additional DS processing gain is obtained without additional bandwidth expansion.

VI. CONCLUSION

In this paper, we proposed an FHSS-MA network employing PN-MWSK and developed two GAs for the conditional error probability, given a hop is hit by K' interfering users. The effect of hits by interfering users hopping to neighboring frequency-hop slots was accurately taken into account. It was demonstrated that employing PN-MWSK significantly improves the network performance compared with employing MFSK. Finally, the effect of imperfect hop timing synchronization was analyzed.

APPENDIX

In this appendix, we derive the MAI term $U_{l,k}^{\mathrm{MAI}}$ for the cases when $0 \leq \tau_k < T_s$ and $-T_s < \tau_k < 0$. We first consider the case when $0 \leq \tau_k < T_s$. Let $c_{k,n}^{m_k} = w_n^{m_k}(a_{k,n}^I + ja_{k,n}^Q)$ and $\tau_k = (L_k + \mu_k)T_c$, where L_k is a nonnegative integer and $0 \leq \mu_k < 1$. Then, by substituting (1) into (5), we have (48), as shown at the bottom of the page, where

$$I \triangleq \int_0^{T_s} h_c(t - mT_c)h_c(t - (n + L_k + \mu_k)T_c)e^{j(2\pi\Delta f_k t + \theta_k)}dt. \tag{49}$$

Note that due to the relative delay of the kth interfering user's signal, compared with the reference user's signal and asynchronous chip timing between different users' signals, $I \neq 0$ only if $0 \leq n < M - L_k$ and $m = n + L_k$ or $m = n + L_k + 1$. Evaluating I for the two cases when $m = n + L_k$ and $m = n + L_k + 1$, (48) can be written as shown in (50) at the top of the next page. Evaluating the integrals in (50) and letting $\rho_k = \Delta f_k T_c$, we obtain

$$\begin{aligned} U_{l,k}^{\mathrm{MAI}} = \frac{\sqrt{E_{s,k}}}{M} e^{j(\pi\rho_k(2L_k+\mu_k+1)+\theta_k)} \cdot \Bigg\{ \Bigg[\frac{\sin(\pi\rho_k(1-\mu_k))}{\pi\rho_k} \cdot \sum_{n=0}^{M-L_k-1} \left(c_{0,n+L_k}^l\right)^* c_{k,n}^{m_k} e^{j(2\pi\rho_k n)} \Bigg] \\ + \Bigg[\frac{\sin(\pi\rho_k\mu_k)}{\pi\rho_k} \cdot \sum_{n=0}^{M-L_k-2} \left(c_{0,n+L_k+1}^l\right)^* c_{k,n}^{m_k} e^{j(2\pi\rho_k(n+(1/2)))} \Bigg] \Bigg\}. \end{aligned} \tag{51}$$

$$\begin{aligned} U_{l,k}^{\mathrm{MAI}} &\triangleq \frac{\sqrt{E_{s,k}}}{T_s} \int_0^{T_s} p_k^{m_k}(t - \tau_k) e^{j(2\pi\Delta f_k t + \theta_k)} p_0^l(t)^* dt \\ &= \frac{\sqrt{E_{s,k}}}{T_s} \int_0^{T_s} \left(\sum_{n=0}^{M-1} c_{k,n}^{m_k} h_c(t - \tau_k - nT_c) \right) \left(\sum_{m=0}^{M-1} c_{0,m}^l h_c(t - mT_c) \right)^* e^{j(2\pi\Delta f_k t + \theta_k)} dt \\ &= \frac{\sqrt{E_{s,k}}}{T_s} \sum_{m=0}^{M-1} \sum_{n=0}^{M-1} \left(c_{0,m}^l\right)^* c_{k,n}^{m_k} I \end{aligned} \tag{48}$$

$$U_{l,k}^{\mathrm{MAI}} = \frac{\sqrt{E_{s,k}}}{T_s}\left\{\left[\sum_{n=0}^{M-L_k-1}\left(c_{0,n+L_k}^{l}\right)^{*} c_{k,n}^{m_k}\cdot\int_{(n+L_k)T_c}^{(n+L_k+1)T_c} h_c(t-(n+L_k)T_c)h_c(t-(n+L_k+\mu_k)T_c)e^{j(2\pi\Delta f_k t+\theta_k)}dt\right]\right.$$
$$\left.+\left[\sum_{n=0}^{M-L_k-2}\left(c_{0,n+L_k+1}^{l}\right)^{*} c_{k,n}^{m_k}\cdot\int_{(n+L_k+1)T_c}^{(n+L_k+2)T_c} h_c(t-(n+L_k+1)T_c)h_c(t-(n+L_k+\mu_k)T_c)e^{j(2\pi\Delta f_k t+\theta_k)}dt\right]\right\}$$
$$=\frac{\sqrt{E_{s,k}}}{T_s}\left\{\left[\sum_{n=0}^{M-L_k-1}\left(c_{0,n+L_k}^{l}\right)^{*} c_{k,n}^{m_k}\int_{(n+L_k+\mu_k)T_c}^{(n+L_k+1)T_c} e^{j(2\pi\Delta f_k t+\theta_k)}dt\right]\right.$$
$$\left.+\left[\sum_{n=0}^{M-L_k-2}\left(c_{0,n+L_k+1}^{l}\right)^{*} c_{k,n}^{m_k}\int_{(n+L_k+1)T_c}^{(n+L_k+1+\mu_k)T_c} e^{j(2\pi\Delta f_k t+\theta_k)}dt\right]\right\} \quad (50)$$

We now consider $U_{l,k}^{\mathrm{MAI}}$ for the case when $-T_s < \tau_k < 0$. Let $\tau_k = -(L_k+\mu_k)T_c$, where L_k is again a nonnegative integer and $0 \le \mu_k < 1$. Setting $t' = t - \tau_k$ in (5) and $\tau_k' = -\tau_k$, we obtain

$$U_{l,k}^{\mathrm{MAI}} = \frac{\sqrt{E_{s,k}}}{T_s}\cdot\int_{\tau_k'}^{T_s+\tau_k'} p_k^{m_k}(t')e^{j(2\pi\Delta f_k(t'-\tau_k')+\theta_k)}p_0^{l}(t'-\tau_k')^{*}dt'. \quad (52)$$

Since the integrand in (52) is zero when $t' < \tau_k'$ or $t' > T_s$, (52) can be written as

$$U_{l,k}^{\mathrm{MAI}} = e^{-j2\pi\Delta f_k\tau_k'}\frac{\sqrt{E_{s,k}}}{T_s}\int_0^{T_s} p_0^{l}(t'-\tau_k')^{*}e^{j(2\pi\Delta f_k t'+\theta_k)}p_k^{m_k}(t')dt'. \quad (53)$$

Note that the integrand of (53) can be obtained by replacing $p_k^{m_k}(t-\tau_k)$ and $p_0^{l}(t)^{*}$ with $p_0^{l}(t'-\tau_k')^{*}$ and $p_k^{m_k}(t')$, respectively, in the integrand of (5). Therefore, it is clear that $U_{l,k}^{\mathrm{MAI}}$ for $-T_s < \tau_k < 0$ can be obtained by replacing $\left(c_{0,n+L_k}^{l}\right)^{*}$, $\left(c_{0,n+L_k+1}^{l}\right)^{*}$ and $c_{k,n}^{m_k}$ with $c_{k,n+L_k}^{m_k}$, $c_{k,n+L_k+1}^{m_k}$, and $\left(c_{0,n}^{l}\right)^{*}e^{-j(2\pi\rho_k(L_k+\mu_k))}$ in (51), respectively, which is given by

$$U_{l,k}^{\mathrm{MAI}} = \frac{\sqrt{E_{s,k}}}{M}e^{j(\pi\rho_k(1-\mu_k)+\theta_k)}\cdot\left\{\left[\frac{\sin(\pi\rho_k(1-\mu_k))}{\pi\rho_k}\cdot\sum_{n=0}^{M-L_k-1}c_{k,n+L_k}^{m_k}\left(c_{0,n}^{l}\right)^{*}e^{j(2\pi\rho_k n)}\right]\right.$$
$$\left.+\left[\frac{\sin(\pi\rho_k\mu_k)}{\pi\rho_k}\cdot\sum_{n=0}^{M-L_k-2}c_{k,n+L_k+1}^{m_k}\left(c_{0,n}^{l}\right)^{*}e^{j(2\pi\rho_k(n+(1/2)))}\right]\right\}. \quad (54)$$

REFERENCES

[1] K. Cheun and K. Choi, "Performance of FHSS multiple-access networks using MFSK modulation," *IEEE Trans. Commun.*, vol. 44, pp. 1514–1526, Nov. 1996.

[2] E. A. Geraniotis, "Multiple-access capability of frequency-hopped spread-spectrum revisited: An analysis of the effect of unequal power levels," *IEEE Trans. Commun.*, vol. 38, pp. 1066–1077, July 1990.

[3] K. Cheun and W. E. Stark, "Probability of error in frequency-hop spread-spectrum multiple-access communication systems with noncoherent reception," *IEEE Trans. Commun.*, vol. 39, pp. 1400–1410, Sept. 1991.

[4] K. Choi and K. Cheun, "Performance of asynchronous slow frequency-hop multiple-access networks with MFSK modulation," *IEEE Trans. Commun.*, vol. 48, pp. 298–307, Feb. 2000.

[5] E. A. Geraniotis, "Noncoherent hybrid DS-SFH spread-spectrum multiple-access communications," *IEEE Trans. Commun.*, vol. COM-34, pp. 862–872, Sept. 1986.

[6] L. L. Yang and L. Hanzo, "Overlapping M-ary frequency shift keying spread-spectrum multiple-access systems using random signature sequences," *IEEE Trans. Veh. Technol.*, vol. 48, pp. 1984–1995, Nov. 1999.

[7] C. M. Keller, "An exact analysis of hits in frequency-hopped spread-spectrum multiple-access communications," in *Proc. Conf. Information Science, Systems*, Mar. 1988, pp. 981–986.

[8] S. H. Kim and S. W. Kim, "Frequency-hopped multiple-access communications with multicarrier on-off keying in Rayleigh fading channels," *IEEE Trans. Commun.*, vol. 48, pp. 1692–1701, Oct. 2000.

[9] S. Glisic, Z. Nikolic, N. Milosevic, and A. Pouttu, "Advanced frequency hopping modulation for spread spectrum WLAN," *IEEE J. Select. Areas Commun.*, vol. 18, pp. 16–29, Jan. 2000.

[10] G. E. Atkin and O. Kucur, "A robust asynchronous multiple-access system using multiple frequencies in AWGN and fading channels," in *Proc. IEEE ISITA*, Nov. 1992, pp. 1151–1154.

[11] M. Soroushnejad and E. A. Geraniotis, "Performance comparison of different spread-spectrum signaling schemes for cellular mobile radio networks," *IEEE Trans. Commun.*, vol. 40, pp. 947–955, May 1992.

[12] W. C. Lindsey and M. K. Simon, *Telecommunication Systems Engineering.* New York: Dover, 1973.

[13] E. A. Geraniotis and M. B. Pursley, "Error probabilities for slow-frequency-hopped spread-spectrum multiple-access communications over fading channels," *IEEE Trans. Commun.*, vol. COM-30, pp. 996–1009, May 1982.

[14] M. B. Pursley, "Performance evaluation for phase-coded spread-spectrum multiple-access communication—Part I: System analysis," *IEEE Trans. Commun.*, vol. COM-25, pp. 795–799, Aug. 1977.

[15] K. S. Gilhousen, I. M. Jacobs, R. Padovani, A. J. Viterbi, L. A. Weaver, and C. E. Wheatley, III, "On the capacity of a cellular CDMA system," *IEEE Trans. Veh. Technol.*, vol. 40, pp. 303–312, May 1991.

[16] E. A. Geraniotis, "Performance of noncoherent direct-sequence spread-spectrum multiple-access communications," *IEEE J. Select. Areas Commun.*, vol. SAC-3, pp. 687–694, Sept. 1985.

[17] M. B. Pursley, D. V. Sarwate, and W. E. Stark, "Error probability for direct-sequence spread-spectrum multiple-access communications—Part I: Upper and lower bounds," *IEEE Trans. Commun.*, vol. COM-30, pp. 975–984, May 1982.

[18] K. Cheun, *Spread-Spectrum Communications: Introduction to Basic Concepts with Emphasis on Direct-Sequence Spreading.* Pohang, Korea: POSTECH Press, 1995.

[19] J. G. Proakis, *Digital Communications*, 3rd ed. New York: McGraw-Hill, 1995.

[20] F. M. Gardner and J. D. Baker, *Simulation Techniques: Models of Communication Signals and Processes*. New York: Wiley, 1995.

[21] M. B. Pursley, "Frequency-hop transmission for satellite packet switching and terrestrial packet radio networks," *IEEE Trans. Inform. Theory*, vol. IT-32, pp. 652–667, Sept. 1986.

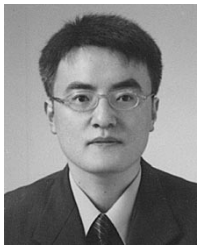

Joonyoung Cho was born in Busan, Korea, in 1971. He received the B.S., M.S., and Ph.D. degrees in electronic and electrical engineering from Pohang University of Science and Technology (POSTECH), Pohang, Korea, in 1993, 1995, and 2003, respectively.

From 1995 to 1998, he was with SK Telecom, Inc., Korea, where he engaged in the development of a W-CDMA modem for an IMT-2000 testbed system. From 1998 to 1999, he worked as a Researcher in the Division of Electrical and Computer Engineering at POSTECH. He is currently with Samsung Electronics Co., Ltd., Korea. His primary research interests are in the areas of spread-spectrum multiaccess communications, turbo codes, and LDPC codes.

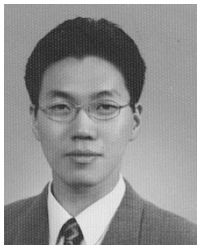

Youhan Kim (S'97) received the B.S. and M.S. degrees in electronic and electrical engineering from Pohang University of Science and Technology (POSTECH), Pohang, Korea, in 1997 and 1999, respectively. He is currently working toward the Ph.D. degree in electronic and electrical engineering at POSTECH.

Since 1997, he has been a Research Assistant at the Department of Electronic and Electrical Engineering, POSTECH, and in 2001, he was a Visiting Student at the University of California, San Diego. His current research interests include spread-spectrum communications, turbo codes, and space–time codes, as well as very large-scale integration (VLSI) design of wireless communications modems.

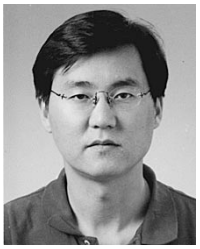

Kyungwhoon Cheun (S'88–M'90) was born in Seoul, Korea, on December 16, 1962. He received the B.A. degree in electronics engineering from Seoul National University, Seoul, Korea, in 1985, and the M.S. and Ph.D. degrees from the University of Michigan, Ann Arbor, in 1987 and 1989, respectively, both in electrical engineering.

From 1987 to 1989, he was a Research Assistant at the EECS Department at the University of Michigan, and from 1989 to 1991, he joined the Electrical Engineering Department at the University of Delaware, Newark, as an Assistant Professor. In 1991, he joined the Division of Electrical and Computer Engineering at the Pohang University of Science and Technology (POSTECH), Pohang, Korea, where he is currently a Professor. He also served as an engineering consultant to various industries in the area of mobile communications and modem design. His current research interests include turbo codes, RA codes, space–time codes, MIMO systems, UWB communications, cellular and packet radio networks, and OFDM systems.